doi:10.1016/j.jmb.2008.04.025 J. Mol. Biol. (2008) 379, 772–786

JMB

Available online at www.sciencedirect.com

ScienceDirect

ELSEVIER

Spontaneous Access to DNA Target Sites in Folded Chromatin Fibers

Michael G. Poirier[1], Malte Bussiek[3], Jörg Langowski[3] and Jonathan Widom[1,2*]

[1]*Department of Biochemistry, Molecular Biology, and Cell Biology, Northwestern University, 2205 Tech Drive, Evanston, IL 60208-3500, USA*

[2]*Department of Chemistry, Northwestern University, 2205 Tech Drive, Evanston, IL 60208-3500, USA*

[3]*Division of Biophysics of Macromolecules, German Cancer Research Center, Im Neuenheimer Feld 580, D-69120 Heidelberg, Germany*

Received 18 February 2008; accepted 7 April 2008
Available online
16 April 2008

Edited by J. O. Bowie

DNA wrapped in nucleosomes is sterically occluded from many protein complexes that must act on it; how such complexes gain access to nucleosomal DNA is not known. *In vitro* studies on isolated nucleosomes show that they undergo spontaneous partial unwrapping conformational transitions, which make the wrapped nucleosomal DNA transiently accessible. Thus, site exposure might provide a general mechanism allowing access of protein complexes to nucleosomal DNA. However, existing quantitative analyses of site exposure focused on single nucleosomes, while the presence of neighbor nucleosomes and concomitant chromatin folding might significantly influence site exposure. In this work, we carried out quantitative studies on the accessibility of nucleosomal DNA in homogeneous nucleosome arrays. Two striking findings emerged. Organization into chromatin fibers changes the accessibility of nucleosomal DNA only modestly, from ~3-fold decreases to ~8-fold increases in accessibility. This means that nucleosome arrays are intrinsically dynamic and accessible even when they are visibly condensed. In contrast, chromatin folding decreases the accessibility of linker DNA by as much as ~50-fold. Thus, nucleosome positioning dramatically influences the accessibility of target sites located inside nucleosomes, while chromatin folding dramatically regulates access to target sites in linker DNA.

Keywords: chromatin; nucleosome; higher-order structure; site exposure; gene regulation

Introduction

Eukaryotic genomes are organized into repeating arrays of nucleosomes that occlude most of the genomic DNA from the many protein complexes required for genome function.[1] How such complexes gain access to their DNA target sites *in vivo* is not known. Genomes encode an intrinsic nucleosome organization in which transcription factor binding sites that need to be accessible have a relatively lower probability of being occluded inside a nucleosome,[2] but these are probabilistic biases only; they do not keep critical target sites nucleosome free.[3–9] Nucleosomal DNA needs to be unwrapped at times to function.[10–13]

Two broad mechanisms that provide access to buried nucleosomal target sites have been characterized. One mechanism involves ATP-dependent nucleosome remodeling factors,[14,15] which disassemble nucleosomes or allow nucleosomes to redistribute their locations in response to changing constellations of DNA binding proteins. These factors are recruited to particular chromatin regions by site-specific DNA binding proteins,[14,16,17] raising the question of how those DNA binding proteins themselves gain access to their own target sites. One idea is that some ATP-dependent remodeling factors may act on nucleosomes ubiquitously, without a requirement for specific binding, thereby rendering

*Corresponding author. Department of Biochemistry, Molecular Biology, and Cell Biology, Northwestern University, 2205 Tech Drive, Evanston, IL 60208-3500, USA. E-mail address: j-widom@northwestern.edu.

Present address: M. G. Poirier, Department of Physics, Ohio State University, 191 West Woodruff Avenue, Columbus, OH 43210-1117, USA.

Abbreviations used: RE, restriction enzyme; cpDNA, core particle DNA; AFM, atomic force microscopy; PL, poly-L-lysine.

chromatin inherently "fluid" for protein binding.[18] Such a ubiquitous activity has not yet been demonstrated *in vivo*.

We focus here on a second mechanism for site accessibility in nucleosomes that is known to occur, is intrinsic to the nucleosomes themselves, and has been implicated in chromatin function *in vivo*. Nucleosomes spontaneously undergo large-scale conformational fluctuations ("site exposure") in which stretches of their wrapped DNA partially unwrap off the histone protein surface, starting from one end. Site exposure provides spontaneous access to the entire nucleosomal DNA length. Access to the more outer stretches of the DNA is particularly rapid (spontaneous opening as often as every ~250 ms)[19] and efficient (the DNA ends are unwrapped as much as ~1%–5% of the time),[20,21] depending on the DNA sequence.[22]

Two lines of evidence suggest that intrinsic nucleosomal site exposure is important for chromosome function *in vivo*. First, one consequence of site exposure is to confer a novel nucleosome-dependent positive cooperativity on the binding of pairs of arbitrary site-specific DNA binding proteins when their DNA target sites are contained within the same nucleosome.[23] This phenomenon occurs *in vivo*[24–26] and is now thought to contribute to cooperativity in transcription factor action, genome-wide.[27] Second, an analysis of rates of DNA repair by photolyase *in vivo* concluded that repair occurs too quickly to be explained by known ATP-dependent remodeling activities and suggested instead that rapid repair is facilitated by intrinsic nucleosome site exposure.[28]

Existing studies characterized the site exposure process only in isolated nucleosomes, but nucleosomes *in vivo* occur in long arrays, which, in physiological conditions, compact into higher-order structures that could hinder site exposure. Indeed, such chromatin compaction occurring *in vivo* has long been proposed to contribute to transcriptional gene silencing by sterically occluding DNA from access to activators or polymerases,[29,30] although a recent study has challenged this interpretation.[31]

Here, we ask how the presence of nucleosome neighbors and concomitant chromatin folding influence site exposure. Two striking findings emerged. First, despite the visible compaction of a model 17-nucleosome chromatin fiber, access to target sites within the central nucleosome is only modestly affected relative to access to the same sites in an isolated nucleosome, and these modest changes range from ~3-fold decreases to ~8-fold increases in accessibility. This means that nucleosome arrays are intrinsically dynamic and accessible even when they are visibly condensed. This finding helps explain how upstream activators may have access to their DNA target sites even in transcriptionally silenced chromatin *in vivo*.[31] Second, in contrast to the modest changes in accessibility it causes within nucleosomes, chromatin folding greatly decreases the accessibility at sites in the linker DNA between nucleosomes, by as much as ~50-fold. Thus, the genome's intrinsic nucleosome positioning ("chromatin primary structure") strongly influences the accessibility of target sites that, on average, are located inside nucleosomes, while chromatin fiber folding ("chromatin secondary structure") regulates access to target sites in regions that, on average, are located in linker DNA.

Results

Reconstitution and characterization of nucleosome arrays

Restriction enzymes (REs) face the same steric problems for access to target sites inside nucleosomes as do many eukaryotic regulators and enzymes and are convenient probes for quantitative analyses of nucleosomal DNA accessibility. Site exposure occurs as a rapid preequilibrium[21]; thus, REs digest nucleosomal DNA at a rate equal to their digestion rate on naked DNA multiplied by the (small) fraction of time that the nucleosomal target sites look like naked DNA, which is the equilibrium constant for exposure of the restriction site in the nucleosomes (Fig. 1). To assess how organization of nucleosomes into compact chromatin fibers influences DNA accessibility, we created two new model systems, having one "test" nucleosome ("mp2") that is flanked by one distinct "mp1" nucleosome on one side only (a dinucleosome) or one mp2 nucleosome flanked by eight other mp1 nucleosomes on each side (a nucleosome 17-mer) (Fig. 2). For the resulting chromatin fibers to have homogeneous nucleosome locations, each mp1 or mp2 nucleosome derives from the 147-bp nucleosome positioning region of sequence 601,[32] with an exactly repeating length of 30 bp of linker DNA separating consecutive nucleosome core particles. Thus, our constructs reproduce essential features of the 177-bp nucleosome repeat systems used in recent biophysical and structural studies in the laboratories of Richmond and Rhodes[33–36] and are novel only in their inclusion of a single distinguishable variant of 601, which allows us to probe accessibility within a particular central nucleosome embedded within a highly positioned nucleosome array.

The nucleosome array reconstitutions were carried out similarly to the work reported in Refs. 33–36, using excess nucleosome core particle DNA (cpDNA) as a histone buffer. When used together with high-affinity nucleosome positioning arrays, the cpDNA allows the preparation of arrays in which every high-affinity sequence is occupied by a nucleosome, without significant aggregation occurring. Optimal dimer reconstitution conditions were determined by titration with increasing concentrations of histone octamer (Fig. 3a). Native gel electrophoresis of the products reveals two distinct shifted single histone octamer-containing bands that converge to a single dinucleosome band by the highest histone octamer concentration used (0.8:1 mass of histone to mass of total DNA, 2.4 mol histone octamer per mole of nucleosome positioning sequence). Products obtained

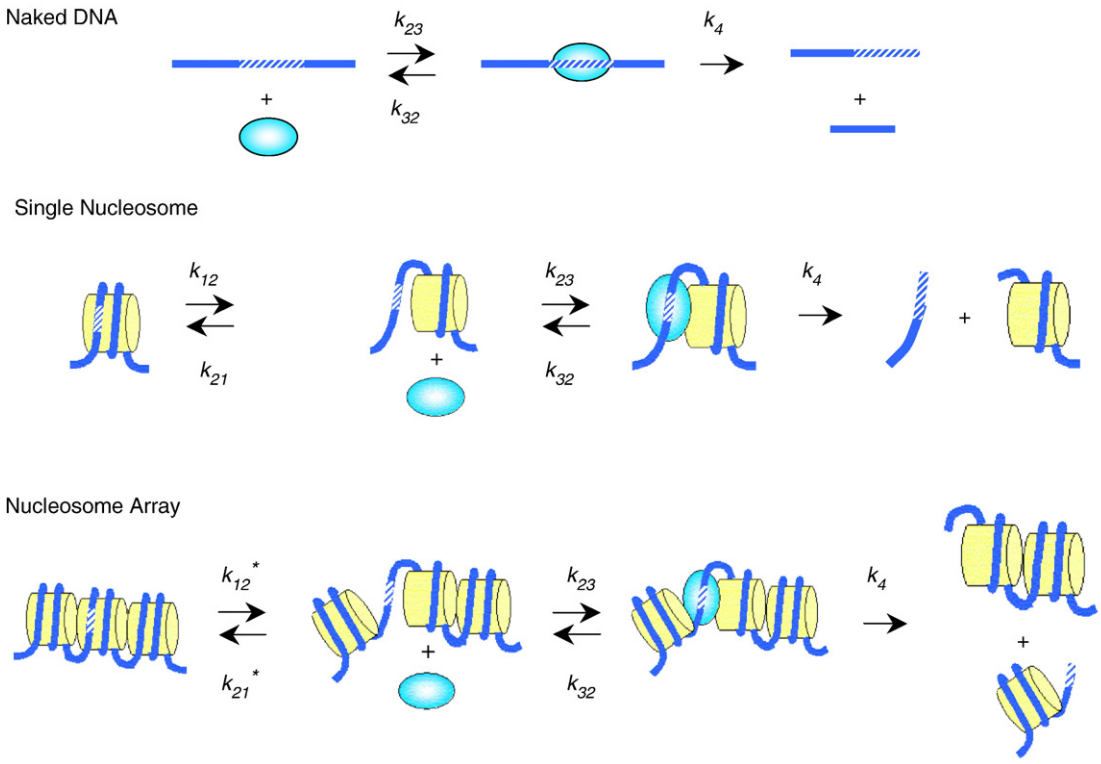

Fig. 1. RE digestion assay for site exposure. k_{12} and k_{21} are the forward and reverse rates of site exposure of a unique DNA site in a single nucleosome, respectively; k_{12}* and k_{21}* are the corresponding rates for exposure of a unique site in a nucleosome array; k_{23} and k_{32} are the rates for RE binding and unbinding, respectively; and k_4 is the rate of RE catalysis. The RE kinetics method determines the equilibrium constant for site exposure, $K_{equ}=k_{12}/k_{21}$ or $K_{equ}=k_{12}^*/k_{21}^*$.

with this highest histone concentration were purified by sucrose gradient centrifugation (Fig. 3b, lane 4).

The purified samples were digested in the linker DNA region with SacI at low enzyme concentration (20 U ml^{-1}) such that naked DNA was fully digested in 1 h, while there was essentially no digestion at sites within a nucleosome to confirm that the products are dinucleosomes and to verify the accuracy of nucleosome positioning within the dinucleosomes. As expected, SacI fully cut the dinucleosomes into two distinct bands (Fig. 3b, lane 5) having mobilities appropriate for mononucleosomes (Fig. 3b, lane 2) containing extra linker DNA. This confirms that the original reconstitutes had two nucleosomes and that essentially no dinucleosome had mispositioned nucleosomes covering the SacI site. Greater than 95% of all DNA was in the mononucleosomes, implying a near-complete saturation of the two nucleosome positioning sequences with histone octamer. Together, these results confirm that the reconstitution procedure produces well-defined, homogeneous dinucleosomes.

We similarly optimized the heptadecamer (17-mer) reconstitutions by titration (Fig. 4a). Native gel electrophoresis reveals a range of mobility shifts that again converge to a distinct band by the highest concentration of histone octamer. This distinct band suggests that the reconstitutions produce a homogeneous

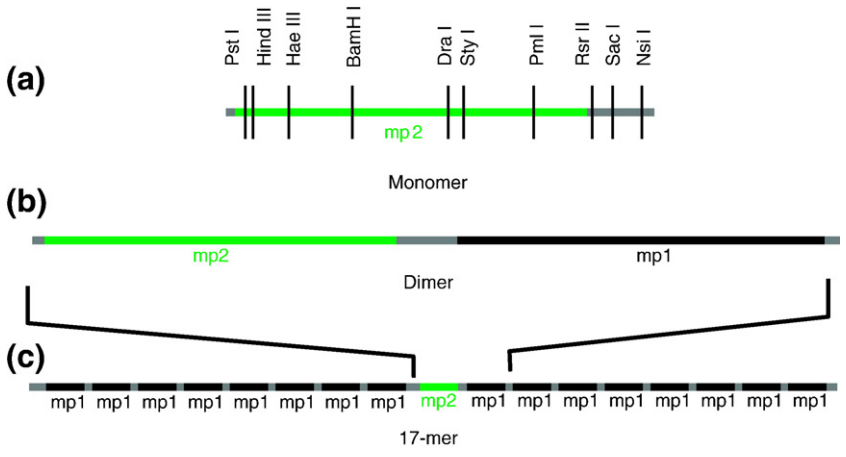

Fig. 2. DNA templates used. The nucleosome positioning sequence mp1 is a variant of positioning sequence 601,[32] while mp2 is a variant of 601.2.[22] mp2 contains many RE recognition sites that are not present in mp1, allowing analysis of accessibility at unique sites within the dimer and 17-mer nucleosome arrays.

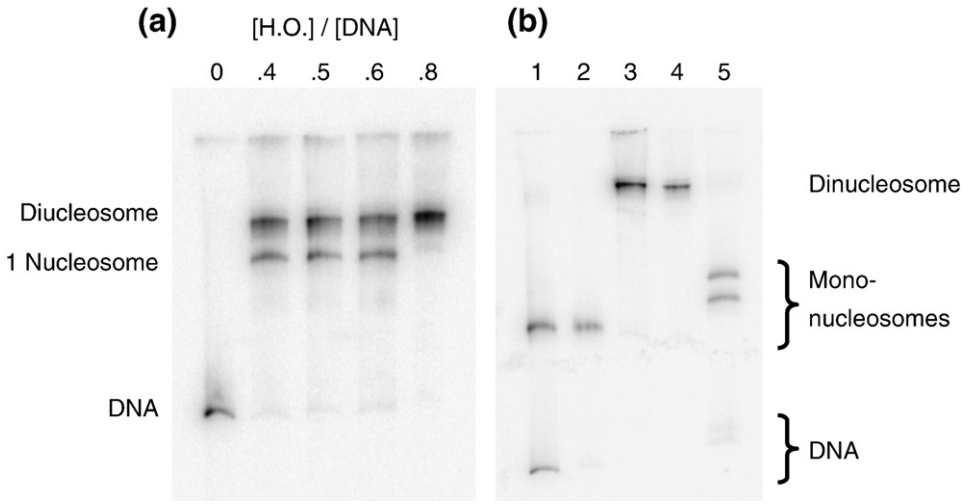

Fig. 3. Reconstitution, purification, and characterization of mononucleosomes and dinucleosomes. (a) Native 5% polyacrylamide gel of dinucleosome template DNA reconstituted with increasing concentrations of histone octamer. The shifts in DNA mobility are due to the formation of one and then two nucleosomes on each DNA. Numbers at the top (0–0.8) indicate the mass ratio (w/w) of histone octamer to total DNA used in the reconstitution reaction in each lane. Total DNA includes both the specific (high-affinity) dinucleosome template DNA plus low-affinity cpDNA competitor present as a histone buffer (see Materials and Methods). The specific template DNA saturates with histone octamer even though the amount of octamer is substoichiometric for the total amount of DNA. (b) Mononucleosome (lanes 1 and 2) and dinucleosome (lanes 3 and 4) reconstitutions before (lanes 1 and 3) and after (lanes 2 and 4) purification on sucrose gradients. Lane 5, purified dinucleosomes after digestion with 20 U ml^{-1} SacI for 1 h. SacI cuts in the linker region, resulting in two bands having gel mobilities similar to those of mononucleosomes (lane 2) and two faint bands from digested naked template DNA (e.g., any template DNA that was not incorporated into nucleosomes). Quantification of these bands shows that greater than 95% of the dinucleosome's positioning sequences are wrapped into nucleosomes.

population of nucleosome arrays; these were then purified by sucrose gradient centrifugation (Fig. 4b).

The array was digested with MluI, which cuts inside each mp1 nucleosome positioning region, to confirm that each mp1 nucleosome positioning region within the 17-mer contains a nucleosome. A trace amount of a 400-bp naked DNA that contains one MluI site was added as an internal reference for the rate of naked DNA digestion. A low concentration of MluI (20 U ml^{-1}) rapidly digested the naked DNA tracer and any naked DNA in the 17-mers, with negligible digestion internal to nucleosomes (Fig. 4c). Quantitative analysis of the digestion showed that the naked DNA digestion fits to a single exponential decay, with a decay rate of 6 min^{-1} (Fig. 4d). The fraction of uncut 17-mer decays with the same rate constant to a final value of 0.5. This means that at least 50% of the 17-mers have 100% of their MluI sites protected by being wrapped into nucleosomes. Since each array contains 16 mp1 sites, at most 0.5 of any of the 16 MluI sites (i.e., at most 3%) are unoccupied by a nucleosome. This in turn implies that at least 97% of all the MluI sites (i.e., at least 97% of the mp1 nucleosome positioning regions) are wrapped into nucleosomes. A similar experiment using StyI digestion showed that 100% of the StyI sites in the mp2 nucleosome positioning sequences are incorporated into nucleosomes (results not shown).

We confirmed the biochemical quality of the 17-mers using atomic force microscopy (AFM) imaging. At low salt concentrations, nucleosome arrays adsorb to the substrate surface in an extended form, allowing individual nucleosomes to be resolved (Fig. 5a and b). AFM images of the 17-mers reveal distinct individual nucleosomes evenly spaced along the DNA template. We imaged 18 molecules: 13 of these had 17 well-resolved nucleosomes each and 3 others appeared to have 17 nucleosomes each, although in each case 2 putative nucleosomes were not well resolved; finally, the other 2 molecules contained 15 or 16 nucleosomes each. In summary, the 18 molecules together contain 306 nucleosome positioning sequences, and the images showed that 299–303 of these 306 positioning sequences were in fact wrapped into a nucleosome. These confirm the biochemical results that greater than 95% of all the nucleosome positioning sequences in these 17-mers are incorporated into a nucleosome.

Higher-order folding of 17-mer nucleosome arrays

Chains of nucleosomes in physiological solution conditions fold into more compact higher-order chromatin structures, even in the absence of the "linker histone" H1 (which is not essential for viability in at least some organisms[37]). *In vitro* biophysical studies on 12-mer nucleosome arrays containing the 601 nucleosome positioning sequence with a 177-bp repeat length—exactly the same as in our 17-mer design—showed these arrays to undergo a reversible compaction in 1 mM Mg^{2+} that resembles the compaction of native chromatin fibers *in vivo* and remains essentially unchanged from 1 to 100 mM Mg^{2+} (Ref. 33).

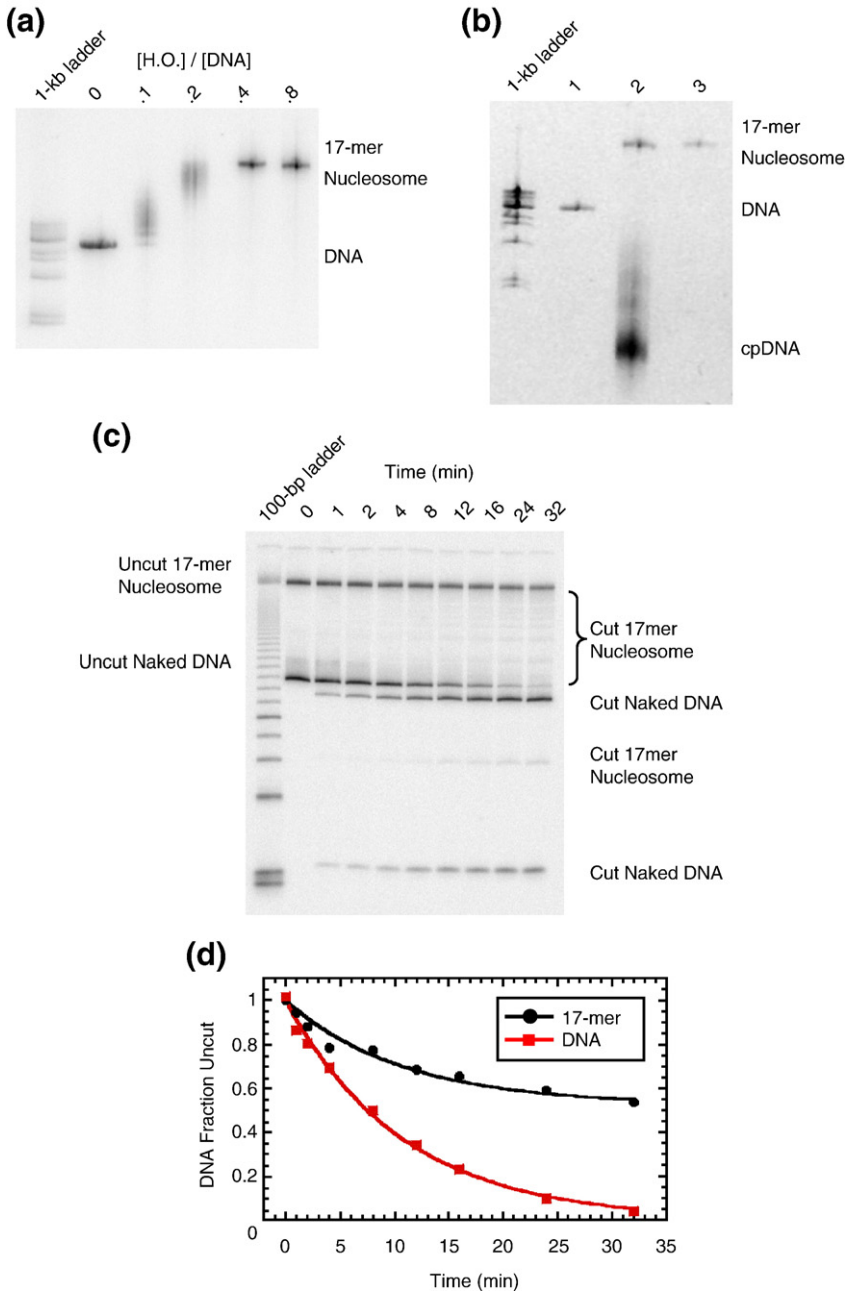

Fig. 4. Reconstitution, purification, and characterization of nucleosome 17-mers. (a) Native gel analysis of 17-mer template DNA reconstituted with increasing concentrations of histone octamer. The mass ratio (w/w) of histone octamer to total DNA used in the reconstitution reaction in each lane is indicated. The decrease in mobility is due to nucleosome formation along the DNA template. The mass ratios 0.1 and 0.2 have a wide range of gel mobilities owing to the inherent heterogeneity of DNA templates that are partially filled with nucleosomes. In contrast, the mass ratios of 0.4 and 0.8 yield a well-defined shift in gel mobility, suggesting that the DNA template is saturated with nucleosomes. (b) Ethidium-stained native gel analysis of the 17-mer DNA template (lane 1) and reconstituted nucleosome array (0.8 histone-to-DNA mass ratio) before (lane 2) and after (lane 3) purification. The sucrose gradient removes the short low-affinity competitor DNA and any aggregates. (c) Native 5% polyacrylamide gel analysis of DNA products from a MluI digestion of purified 17-mer nucleosomes mixed with naked DNA. The 17-mer contains 16 MluI sites, and the naked DNA contains a single MluI site. (d) Quantification of results from (c) showing the fraction of naked DNA and the nucleosome 17-mer remaining uncut, as a function of time. The curves show best fits to the appropriate exponential decays (see Materials and Methods). These results show that 0.03 of the positioning sequences are not incorporated into nucleosomes (i.e., that 97% of all positioning sequences in these nucleosome 17-mers are wrapped into nucleosomes).

Thus, 12-mer arrays are already maximally compacted by 1 mM Mg^{2+}, and they maintain this compaction in the 5–10 mM Mg^{2+} concentration range in which REs are active. While it is conceivable that the nucleosome arrays could become even more highly compacted for Mg^{2+} concentrations greater than 100 mM, such conditions are too extreme to be of physiological relevance. Thus, we, as well as others,

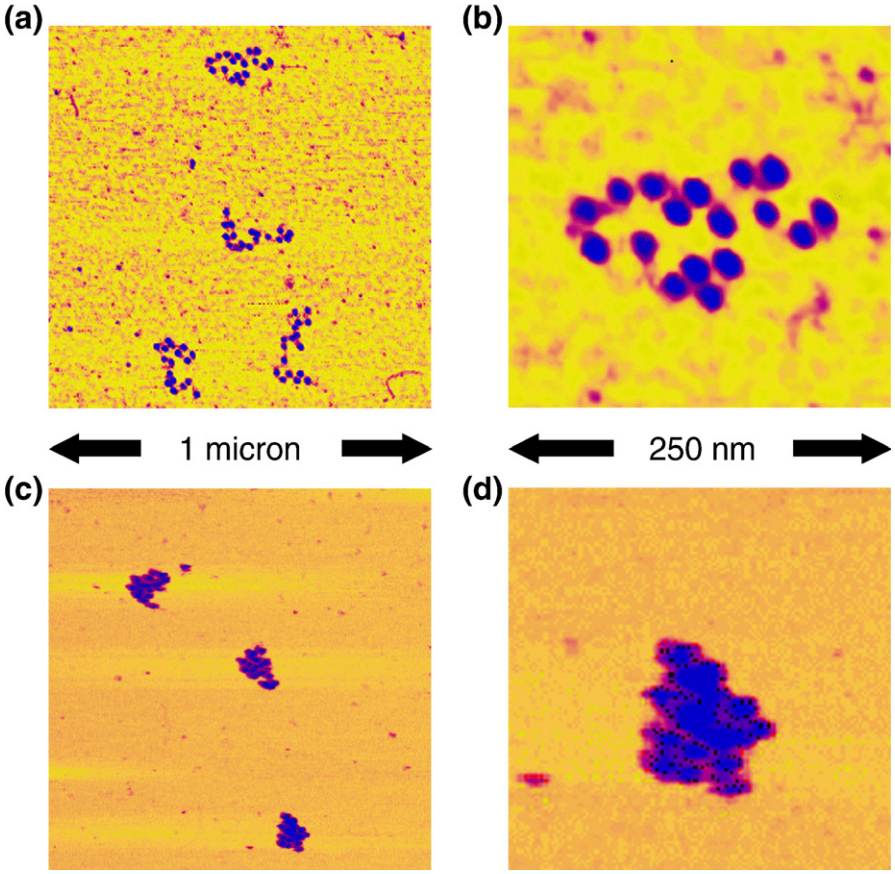

Fig. 5. AFM images of nucleosome 17-mers. (a and b) Purified nucleosome 17-mers adsorbed onto mica in 0.2× TE (which causes them to adopt extended conformations) and imaged in air. (b) Zoom (4×) of the upper array in (a). These and additional images confirm the biochemical results showing that the 17-mers are greater than 95% saturated with nucleosomes. (c and d) 17-mers adsorbed in 0.5× TE plus 1 mM $MgCl_2$ (which allows them to compact) and imaged in that buffer. (d) Zoom (4×) of the lower array in (c). As expected, the arrays fold into more compact structures in the presence of $MgCl_2$.

have focused our analyses on the quasi-physiological Mg^{2+} concentration range of 1–10 mM, in which the arrays are as compacted as they will ever be for any reasonable Mg^{2+} concentration. Because of the similarities in design, we expected that our 17-mer arrays would undergo a similar Mg^{2+}-dependent folding. Indeed, AFM images of our 17-mers confirm that, like the 12-mer arrays, they are highly compacted already by 1 mM Mg^{2+} (Fig. 5c and d). Our RE digestion assays were carried out in 5–10 mM Mg^{2+} and thus probed the effects of both the presence of nucleosome neighbors together with this concomitant chromatin folding.

Site accessibility in folded nucleosome arrays

Having established a protocol for assembly of dinucleosomes and nucleosome 17-mers, we next used the RE accessibility assay to quantify how the presence of nucleosome neighbors and concomitant chromatin folding influence accessibility inside the test nucleosome. For the RE assay as originally developed, one measures the rate of digestion at a given nucleosomal DNA target site relative to the rate of digestion of the same site as naked DNA, scaled for differences in the enzyme concentrations used. The ratio of these scaled digestion rates yields the equilibrium constant for site exposure of that site in the nucleosome (i.e., the equilibrium fraction of time that a given nucleosomal DNA target site is as available to another protein as is the same site in naked DNA). The experiments are carried out in a rapid preequilibrium regime (rapid rewrapping of site-exposed DNA compared with the rate of RE binding), where the REs serve as neutral reporters of spontaneous nucleosomal site exposure.[21,38] Strictly speaking, the assay measures the "effective accessibility," which could differ from true accessibility if the properties of DNA transiently unwrapped off the nucleosome surface differ from true naked DNA. Full experimental validation of the assumptions behind this assay had been published previously.[21,38]

To apply this procedure for the present case, we would measure rates of digestion of a test nucleosome relative to the same sequence as naked DNA, for the test nucleosome present first in a mononucleosome and then again in a dinucleosome or in a 17-mer. However, in pilot studies, we observed that the rate of digestion at sites inside the test nucleosome in the arrays was similar to that of digestion at the same sites in mononucleosomes. This feature allowed us to improve our experimental design to

more accurately measure the effects of nucleosome neighbors and concomitant chromatin folding. Rather than measure the mononucleosome and array sample independently relative to naked DNA, we instead added the mononucleosomes to the array sample together in the same tube and measured their accessibility directly relative to each other, in the same reaction at the same time.

We used this approach to evaluate the equilibrium accessibility at seven sites spanning the length of the

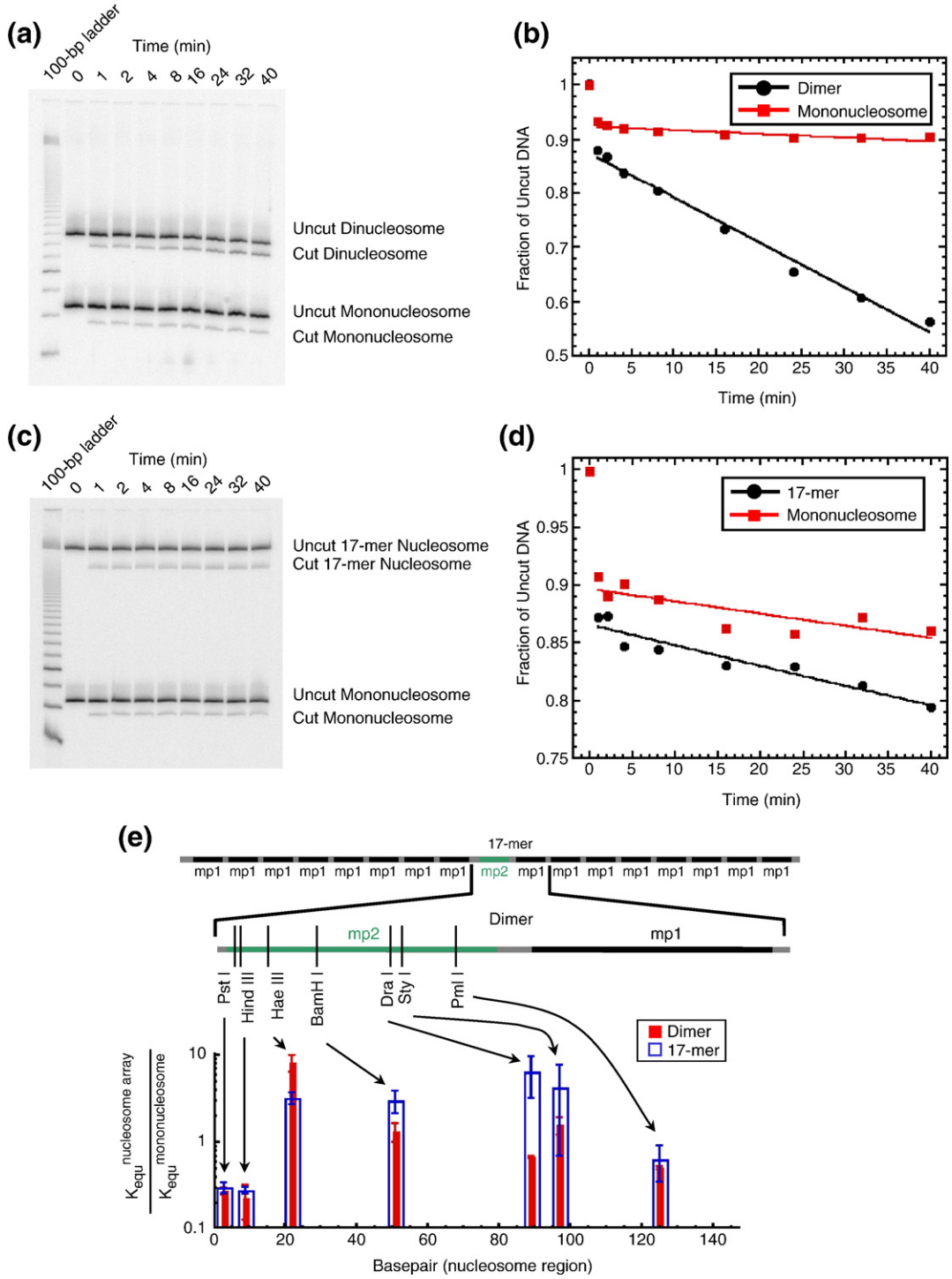

Fig. 6. Site exposure in dinucleosomes and nucleosome 17-mers measured relative to mononucleosomes. (a) Native gel analysis of DNA products from HaeIII digestions of a mixture of purified dinucleosomes and mononucleosomes; times of digestion (in minutes) are indicated. (b) Quantification of the fraction of uncut DNA from (a), fit with an exponential decay (see Materials and Methods). (c and d) As in (a) and (b) except that purified nucleosome 17-mers were used in place of dinucleosomes. (e) Summary of site accessibilities in dinucleosomes and nucleosome 17-mers, measured relative to accessibilities in mononucleosomes, for sites spanning the test nucleosome. Averages and standard deviations ($n = 2$ or 3) are shown.

test (mp2) nucleosome (Fig. 6a–d). As shown previously,[21,38] rapid mixing of the nucleosomes or nucleosome arrays into the RE digestion buffer causes up to 10% of the nucleosomes to fall apart at the zero time point of the digestion reaction; the resulting naked DNA is effectively instantly digested. We handle this in the kinetic analysis by omitting the first time point. With the nucleosome array constructs analyzed here, any nucleosome dissociation is dominated by loss of the test nucleosome itself,

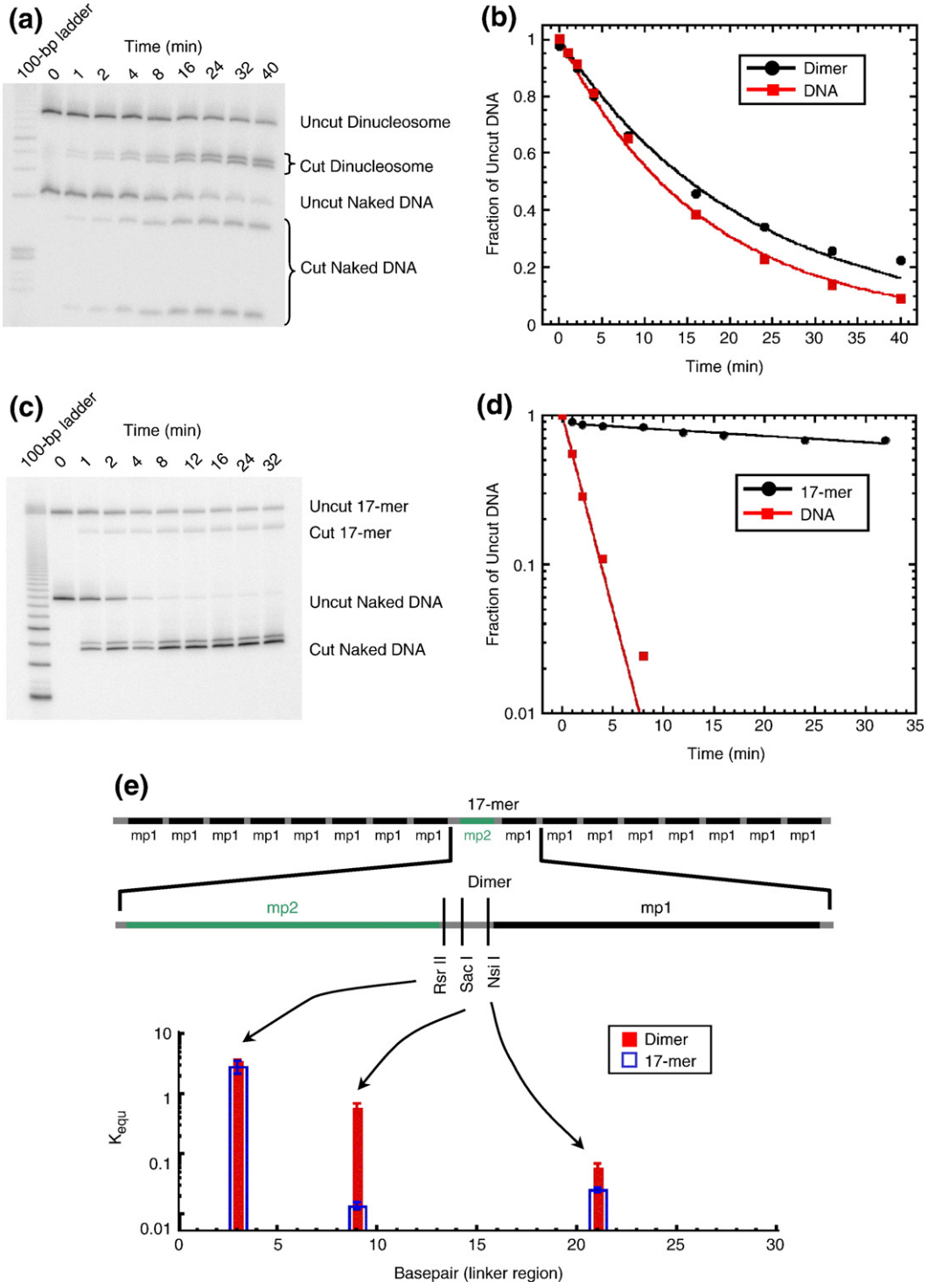

Fig. 7. Site exposure in linker DNA within dinucleosomes and nucleosome 17-mers measured relative to naked DNA. (a) Native gel analysis of DNA products from SacI digestions of a mixture of purified dinucleosomes and naked DNA; times of digestion (in minutes) are indicated. (b) Quantification of the fraction of uncut DNA from (a), fit with an exponential decay. (c and d) As in (a) and (b) except that purified nucleosome 17-mers were used in place of dinucleosomes. (e) Summary of site accessibilities in dinucleosome and nucleosome 17-mer linker DNA, measured relative to accessibilities in naked DNA, for sites spanning one linker DNA region. Averages and standard deviations (n=2–5) are shown.

rather than the flanking nucleosomes, which, because of the test nucleosome's engineered sequence changes, is lower in affinity (stability) compared with the flanking nucleosomes (for details, see Materials and Methods); in addition, as just explained, loss of the test nucleosome is accommodated in our analysis by omitting the first digestion time point. At most 3% of the nucleosomes flanking the test nucleosome dissociate (see Materials and Methods); thus, gaps in the nucleosome array surrounding the test nucleosome occur with negligible probability and do not affect the measured accessibilities. Quantitative analysis of the reaction kinetics reveals that the presence of one or many nucleosome neighbors—with concomitant folding of the nucleosome array for the case of the 17-mer arrays—causes detectable but modest changes in equilibrium accessibility (K_{equ}) of target sites throughout the test nucleosome (Fig. 6e). These changes in equilibrium accessibility due to the nucleosome neighbors range from ~3-fold decreases to ~8-fold increases, which are small in comparison with the 10^3- to 10^6-fold quantitative effects on accessibility of wrapping 601 DNA into nucleosomes in the first place.[22]

Site accessibility in linker DNA

We used the same approach to quantify the effects of nucleosome neighbors and concomitant chromatin folding on the accessibility of target sites in linker DNA, except that in this case we used naked DNA as the internal reference, yielding linker accessibility relative to naked DNA. We made measurements at three sites spanning the 30-bp linker DNA (Fig. 7a–d). Strikingly, quantitative analysis of the reaction kinetics in this case revealed that, in conditions that stabilize higher-order folding of the nucleosome arrays, the presence of one or many nucleosome neighbors strongly influences the accessibility of sites inside the linker: accessibility is reduced by as much as ~50-fold at a site in the middle of the linker in the 17-mer arrays (Fig. 7e).

These and other observations also imply that any self-association (aggregation) of the nucleosome arrays, which could be caused by the Mg^{2+} in the RE buffers,[39] is not significantly influencing the observed site accessibilities. If aggregation significantly influenced the digestion kinetics, this should lead to non-single exponential behavior, with many nucleosomes resistant to digestion, and to comparably large decreases in accessibility for all sites in linker DNA or nucleosomes—all of which predictions are contrary to observation (as discussed above; also, see Materials and Methods). Moreover, our results show that REs digest nucleosomal DNA within arrays at rates that are similar to those for single nucleosomes, while we showed in previous studies that site exposure in single nucleosomes occurs to a similar quantitative extent regardless of whether the solutions contain Mg^{2+} or not,[20] and we proved that nucleosomes undergoing spontaneous site exposure in solutions lacking Mg^{2+} are not aggregated.[19] Based on all these considerations, we conclude that any aggregation of the nucleosome arrays in our experiments negligibly influences the measured relative equilibrium accessibilities.

Discussion

Two results from this study stand out. First, surrounding a nucleosome with many neighbors on each side in a chromatin fiber, with concomitant higher-order compaction of that fiber, only causes a modest change in accessibility of sites within the central nucleosome relative to the accessibility of the same sites in a single isolated nucleosome. Moreover, these modest changes in accessibility that do exist range from ~3-fold decreases to ~8-fold increases. This means that folded nucleosome arrays are intrinsically dynamic to an extent that target sites even in the least accessible locations in a nucleosome are nevertheless constantly but transiently accessible. This finding provides one explanation for how upstream activators have access to their DNA target sites even in transcriptionally silenced chromatin *in vivo*.[31]

Second, in contrast to the modest changes it causes in accessibility of nucleosomal sites, higher-order compaction of the chromatin fiber dramatically influences the accessibility of certain sites in the linker DNA: the accessibility of the SacI site in the middle of the linker DNA in a chromatin fiber, relative to the same site in naked DNA, is reduced by as much as ~50-fold. Accessibility at other sites in the linker is less strongly decreased (NsiI) or even slightly increased (RsrII) by the existence of neighbor nucleosomes.

We emphasize that the RE kinetics method quantifies the DNA accessibility for the specific RE used in the experiment. Details of the size and shape of the enzyme and how it binds will differ between enzymes and can in principle influence the apparent accessibilities. Nevertheless, for digestion inside the nucleosome, enzyme-specific differences appear to be small in comparison with the position-dependent protection against binding of any protein, which is conferred by the nucleosome: accessibilities decrease quite progressively from the ends into the middle of the nucleosome, despite the use of many unrelated REs and other site-specific DNA binding proteins.[22] Nevertheless, the distinct effects on accessibilities on nearby sites in linker DNA, observed here, may be attributable in some measure to enzyme-specific differences in the requirements for a site to become accessible. In that case, our findings would indicate that chromatin folding can specifically block certain DNA binding proteins while permitting others to bind in the same stretch of linker DNA.

Structural determinants of DNA target site accessibility in chromatin

Many nucleosomes *in vivo* are relatively well positioned: they have a high probability of occupying particular genomic locations.[2,22,40] It is now under-

stood that these preferred locations are in part encoded directly in the genomic DNA sequence and are in part a consequence of competition with other site-specific DNA binding proteins.[2,27,41–44] In this context, what is the meaning of our new findings about relative accessibility of nucleosomal and linker DNA in chromatin fibers?

One conclusion is that the detailed location of a nucleosome along the genome, at a given point in time, is a dominant determinant of DNA site accessibility. DNA sites that are located far inside a nucleosome (e.g., near the middle) are as much as 10^3–10^5 times less accessible than are sites near the ends of the nucleosome or in linker DNA. For typical site-specific DNA binding proteins, the resulting *effective* dissociation constant for binding to a target site in the middle of the nucleosome is likely to greatly exceed the actual free concentration of the protein. In this case (i.e., whenever free concentrations are low compared with the effective dissociation constant), a 10^3- to 10^5-fold decrease in accessibility for a site in the middle of the nucleosome translates directly to a comparable decrease in the expected *occupancy* of a typical regulatory protein at that target site. Compared with that very large potential decrease in occupancy attributable to the detailed location of a nucleosome itself, additional ~3- to 8-fold (negative or positive) changes in accessibility attributable to organization of a nucleosome into a compacted chromatin array are plainly of more modest significance.

In contrast, for sites in the middle of linker DNA regions, the opposite situation obtains. Here, accessibility is intrinsically high, yet proximity to neighboring nucleosomes coupled to chromatin folding can decrease that accessibility dramatically, by at least ~50-fold. If, as seems plausible, *in vivo* concentrations and DNA binding affinities of a regulatory protein are tuned for significant but partial occupancy on naked DNA, then the occupancy of such a protein on a target site in linker DNA in chromatin will sensitively depend on the folded state of the chromatin fiber and on the presence or absence of other nucleosomes immediately nearby. Large effects on accessibility and occupancy at such genomic locations are to be expected.

Finally, for sites that are located near the ends of the nucleosome, the situation is more complex. The intrinsic accessibility of such sites in an isolated nucleosome is reduced relative to naked DNA but is much less reduced than for sites near the middle of the nucleosome. The extent of reduction of accessibility depends sensitively on the particular DNA sequence and may be as little as ~20-fold for sites near the end of an intrinsically less stable nucleosome.[21] Few-fold effects of changing accessibility on top of that, due to placement in a chromatin fiber and concomitant chromatin folding, may lead to few-fold changes in occupancy. Whereas few-fold changes in occupancy for sites near the middle of the nucleosome may be of modest consequence, because the occupancy may be so low to begin with, comparable changes when occupancy is higher may be of great significance. The phenomena of dosage compensation and haploinsufficiency diseases remind us of the potential significance of even 2-fold effects on gene expression.

In summary, for chromatin fibers composed of a repeated array of nucleosome core particles connected by typical-length segments of linker DNA, the detailed positioning of nucleosomes along the DNA is a dominant determinant of accessibility, while the presence of nucleosome neighbors and concomitant chromatin folding will subtly but significantly affect the accessibility of sites near the periphery of a nucleosome (especially for nucleosomes whose DNA end is not too stably wrapped) and will greatly affect the accessibility of regions in linker DNA.

Regulated DNA accessibility in chromatin fibers

Earlier studies showed that the accessibility of target sites within individual nucleosomes is quantitatively influenced by the acetylation patterns of the core histone tail domains.[45,46] Here, we are concerned with influences on target site accessibility arising from the organization of isolated nucleosomes into a repeating array in which each nucleosome is flanked with many neighbors and in which the entire chain of nucleosomes then folds into a more compact higher-order structure. Like other recent studies,[33,34,47,48] our work has addressed chromatin folding as it occurs in the absence of other chromatin-associated proteins. The "linker histone" H1 is a chromatin-associated protein of particular interest since it can occur in nearly stoichiometric amounts compared with nucleosomes. Even though histone H1 has been implicated in stabilizing higher-order chromatin folding,[49] studying the accessibility of chromatin fibers lacking histone H1 is justified since the chromatin fibers visibly compact even without histone H1 and the single yeast gene for histone H1, which has significant homology to higher cell histone H1, is not essential for viability.[37] In higher cells, a regulated higher-order chromatin folding, which might be facilitated by the regulated binding and unbinding of histone H1, might play more important roles, which are not revealed in our study. Although questions concerning the nature and biological roles of higher-order chromatin folding remain unresolved, useful conclusions may already be drawn.

First, a dominant role for nucleosome positioning on accessibility of DNA target sites *in vivo* is supported by many recent studies.[41,50–52] Importantly, however, nucleosome positions themselves are regulated. While nucleosome positions *in vivo* are influenced by the underlying genomic sequence,[2] they are also influenced by competition with the constellation of competing site-specific DNA binding proteins.[2,41,43,44] When this constellation changes, nucleosomes redistribute their locations in a manner that depends both on the concentrations as well as affinities of the competing proteins and on the underlying intrinsic landscape for nucleosome

positioning. The action of remodeling factors and existence of linker DNA can be required to facilitate the redistribution of nucleosome positions.[14,15,53]

Beyond regulated nucleosome positioning, our results suggest that regulated chromatin folding may meaningfully influence target site accessibility *in vivo* too. A recent study of chromatin folding *in vitro* established that acetylation of histone H4 lysine 16 (K16) specifically destabilizes the higher-order folding of chromatin fibers.[47] Our studies utilized histone octamers purified from chicken erythrocytes, which are transcriptionally inert and have minimally acetylated histones.[54] Thus, our results reflect a more stable form of the chromatin fiber.[45] Any destabilization of the fiber caused by specific acetylation of histone H4 K16 would only reduce the magnitudes of the already modest changes in accessibility that we observed. Thus, we expect that regulated folding or unfolding of the chromatin fiber may have little role in regulating access to sites in the middle of a nucleosome, where accessibility is always strongly reduced. Nevertheless, regulated folding may play an important biological role by modulating access to sites near the ends of a nucleosome or in linker DNA, where accessibility is intrinsically much greater.

Materials and Methods

DNA constructs

The DNA templates used are tandem repeats of variants of the 601 high-affinity nucleosome positioning sequences 601[32] and 601.2[22] with exactly 30 bp of linker DNA length between each 147-bp-long nucleosome, yielding a repeat length of 177 bp. Eight base changes were made within 601 to give the sequence mp1, and two base changes were made within 601.2 to give the sequence mp2. With these sequence changes, there were eight RE sites within mp2 across the nucleosome that are not present within mp1. The mp1 sequence was prepared by three rounds of PCR amplification. The first PCR amplification used the 601 sequence as template with the primers AGCCGCTCAATTGGTCGTAGCAAGCTCTACCACCGCTTAAACGCACGTAAGGGCTGTCCCCCGCG and TACATGCACAGGATGTATATATCTGACGCGTGC-CTGGAGACTGGGGAGTAATC-CTCTTGGCGGTT. The product was gel purified and used as the template for the second round of PCR amplification with the primers GCATCCCGCCCT-GGAGAATCTTGGTGCCGA-AGCCGCTCAATTGGTCGTAGCAA and CTTTGATCAAGA-TCTCCCGAGTTCAATACATGCACAGGATGTATATATCTGACGCG. This product was also gel purified and used as the template for the third round of PCR amplification with the primers TTGACGACCGGAATTCAGAGCTCCTCGGGATGCATCCCGCCCTGGAGAATC and CTCCTTATCCCAAGCTTTGATCAAGATCTCCCGAGTTCAATAC. This final product was gel purified and cloned into the multiple cloning site of pUC19 between the EcoRI and HindIII sites, yielding plasmid pMP1. The mp1 sequence is flanked on both sides by the asymmetric AvaI site CTCGGG and by the EcoRI and SacI sites on one side and BclI and BglII on the other.

A tandem repeat of eight mp1 sites was prepared by ligation of AvaI-cut mp1 fragment. The single mp1 DNA insert was cleaved out of pMP1 with AvaI; the mp1 fragment and the linearized vector were gel purified. The mp1 fragment was ligated for 1 min with Quick Ligase (Qiagen), and the linearized vector was then added and allowed to ligate for an additional 5 min. The resulting plasmid was transformed into DH5α cells. Repeats of up to 12 were cloned. The cloned mp1 repeats were sequenced; the longest insert that could be completely sequenced was the octamer of mp1.

The mp2 sequence was also made by three rounds of PCR amplification. The first PCR amplification used the 601.2 sequence as the template with the primers GACGAGGTGCGG-GGATGATCACTGCAGAAGCTTGGTGCCGGGGCCGC and TGTATATATCTGACACGTGCCTGGAGACTAGGGAGTAATCCCCTTGGCGTTTAAAACGCG. The PCR product was gel purified and used as the template for the second round of PCR amplification with the primers AGGCGCCCCGGAATTCCGGTTGACGAGGTGCGGGGATGATCA and CTCGTCCTTATCGAGCTCGGTCCGACAGGATGTATATATCTGACACGTGCCTGGAGACTAG. This PCR product was gel purified and used as the template for the third round of PCR amplification with the primers AGGCGCCCCGGAATTCCGGTTGACGAGGTGCGGGGATGATCA and CGCCACACATGCATGCAGATCTATGTCGGGCTCGTCCTTATCGAGCTCGGTC. This final product was cloned into the multiple cloning site of pUC19 between the EcoRI and SphI sites, yielding plasmid pMP2. The mp2 sequence is flanked on one side by the EcoRI and BclI sites and on the other side by the SacI and BglII sites.

The dinucleosome DNA template was made by cloning a single mp1 sequence adjacent to the mp2 sequence between the SacI and BglII sites. This strategy yields a 30-bp-long linker DNA between the two positioning sequences, in plasmid pMP2_MP1. The heptadecamer (17-mer) DNA tandem repeat was made by cloning an mp1 8-mer between the EcoRI and BclI sites and (separately) between the SacI and BglII sites. This created a tandem repeat of 17 nucleosome positioning sequences with eight mp1 sequences, then one mp2 sequence, and then eight mp1 sequences, all spaced by exactly 30 bp of linker DNA, in plasmid pMP17.

Histones

Histone octamer was purified from chicken erythrocytes as described in Ref. 55.

Mononucleosome reconstitutions

Mononucleosomes were reconstituted and purified as described in Ref. 22. Briefly, the DNA template used for reconstitutions was PCR amplified from plasmid pMP2 with the primers TGATCACTGCAGAAGCTTGGTGC and GAGCTCGGTCCGACAGGATGT. The PCR product was purified by reversed-phase HPLC and 5′ end-labeled with ^{32}P using T7 kinase, which was then heat denatured. Reconstitutions were done by double dialysis[56] with 1 μg of radiolabeled mp2 DNA, 4 μg of cold (unlabeled) mp2 DNA, and 4 μg of chicken erythrocyte histone octamer. This incorporated about 80% of the mp2 DNA into nucleosomes (Fig. 3b, lane1). The reconstituted mononucleosomes were then purified on a sucrose gradient[32] to remove the free DNA and aggregates (Fig. 3b, lane2).

Nucleosome array reconstitutions

The dimer DNA template was prepared for reconstitution by PCR amplification using pMP2_MP1 template

DNA with the primers GAATTCCGGTTG-ACGAGGTGC and GCTTGCATGCAGATCTCCCG. The product was purified by reversed-phase HPLC and ^{32}P end-labeled using T7 kinase. The 17-mer DNA template was cut out of pMP17 with EcoRI and HindIII. The vector was cut into many pieces with DdeI, and the 17-mer was then purified away from these pieces by agarose gel electrophoresis. The purified 17-mer DNA was dephosphorylated using Antarctic Phosphatase (NEB), which was then heat killed, and then the DNA was ^{32}P end-labeled using T7 kinase.

Nucleosome arrays were reconstituted onto these DNAs by double dialysis using radiolabeled dimer or 17-mer DNA templates, chicken erythrocyte histone octamer, and cpDNA, which is used to buffer the reconstitutions so that the arrays saturate with positioned nucleosomes without substantial aggregation.[33,35] The reconstitutions were done in a volume of 50 μl in lab-made dialysis buttons.[56] The mass ratio of histone octamer to total amount of DNA used to fully reconstitute the arrays was 0.8. The buttons were inserted into a large dialysis tubing filled with 80 ml of 0.5× (v/v) TE [10 mM Tris, pH 8.0, and 1 mM ethylenediaminetetraacetic acid (EDTA)], 2 M NaCl, 1 mM benzamidine hydrochloride, and 0.5 mM PMSF (phenylmethylsulfonyl fluoride). The large dialysis tubing was placed into 4 l of 0.5× TE, 1 mM benzamidine hydrochloride, and 0.5 mM PMSF. This was dialyzed for 6 h at 4 °C, and then the 4 l was changed and dialyzed overnight at 4 °C. The reconstituted nucleosome arrays were then collected from the dialysis buttons and purified on sucrose gradients.

Biochemical characterization of nucleosome arrays

The dimer reconstitutions were assayed by gel shifts on 4% polyacrylamide gels in 0.3× (v/v) TBE (90 mM Tris–borate and 2 mM EDTA). The dinucleosome reconstitutions display two distinct gel shifts, which correspond to the formation of a first nucleosome followed by a second on each template DNA. This allows us to determine the reconstitution conditions that incorporate ~100% of the positioning sequences into nucleosomes. To confirm this, we digested the dinucleosomes with SacI at a concentration of 20 U ml^{-1}, which cuts in the linker region between the mp1 and mp2 positioning sequences. This converts dinucleosomes into two mononucleosomes with little free DNA (Fig. 3b, lane 5). The difference in gel mobility of the two single nucleosomes is due to the difference in length of DNA that extends out from the nucleosome.

The 17-mer (Fig. 4a) reconstitutions were assayed by gel shifts on mixed 2% polyacrylamide plus 1% agarose gels in 0.2× TB (90 mM Tris–borate). Unlike the dimer reconstitutions, the partially reconstituted heptadecamer gel shift bands were not all distinguishable and instead appeared as a smear (Fig. 4a, lanes ".1" and ".2"). It is therefore difficult from the gel shift assay alone to be sure that the arrays are saturated with nucleosomes. However, the gel shift at higher concentrations of histone octamer is a tight, well-defined band, suggesting that those arrays are saturated. MluI digestions of the reconstituted 17-mers relative to naked DNA having a single MluI site were used to quantify the number of positioning sequences that were incorporated into nucleosomes in the 17-mer reconstitutes (Fig. 4b). The digestion kinetics of the 17-mer reconstitutes and naked DNA were measured in the same reaction volume. Time points were taken by quenching 10 μl of the digestion with 20 mM EDTA. Subsequently, the histone octamers were removed with 1 mg/ml of proteinase K and 0.02% SDS. Aliquots were analyzed on 5% polyacrylamide gel using a PhosphorImager (Molecular Dynamics). Image Quant software was used to determine the amount of uncut 17-mer and naked DNA (Fig. 4c). The naked DNA digestion (Fig. 4d, red) is fit with a normalized exponential, exp $(-k0*t)$, where $k0 = 6$ min^{-1}. The 17-mer nucleosome digestion is fit with the function $C + (1-C)$ exp $(-t*6$ min$^{-1})$, where $C = 0.5$. The value C is the fraction of arrays that has all 16 MluI sites protected from digestion. It follows that 0.03 (3%) of the positioning sequences are not incorporated into nucleosomes and that, therefore, 97% of the positioning sequences in the 17-mer reconstitutes are wrapped into nucleosomes.

Array imaging by AFM

AFM imaging was used to confirm that the arrays were saturated and to determine the folded state in various conditions. Imaging was done in air and in liquid using Multimode AFM (Digital Instruments) operated in tapping mode. Freshly cleaved mica was pretreated with 30 μl of an aqueous solution of poly-L-lysine (PL, Sigma) at a concentration of 10 μg ml^{-1}. Following a 30-s incubation, unbound PL was removed by rinsing the mica disc with 3 ml of Millipore purified water followed by drying under a nitrogen stream. The arrays were diluted at a concentration of ~0.15 nM in 0.5× TE or 0.2× TE, pH 7.5, either with or without additional salt (see the text). A total of 30 μl of the array solution was placed on the PL mica. For scanning directly in the adsorption buffer, silicon nitride probes (type NP-S20, Veeco Instruments) were used at a drive frequency of ~9.0 kHz and a set point of 0.3–0.4 V. This method was chosen to verify the condensed state of the arrays in the presence of $MgCl_2$, in order to circumvent the need of rinsing with water. The arrays were also scanned in air to reliably distinguish individual nucleosomes in extended array conformations at low salt conditions. For this, the mica disc was washed carefully with 2.0 ml of Millipore water after a 1-min incubation with the array solution. The disc was then dried with nitrogen and subsequently scanned using etched silicon probes (type NHC, Nanosensors) at drive frequencies of 280 to 320 kHz and a set point of 2.0–2.2 V. The images were recorded both in solution and in air at a scan diameter of 2×2 μm, a scan rate of 1–2 Hz, and a resolution of 512×512 pixels. With the use of Nanoscope IIIa software (version 5.12r3, Digital Instruments), recorded images were flattened and areas of the imaged fields were zoomed for counting nucleosomes and for presentation.

RE kinetics method for nucleosomal DNA

The RE kinetics method[21,38] was used to quantify DNA accessibility, defined as the equilibrium constants of site exposure, $K_{equ} = k_{12}/k_{21}$, the equilibrium fraction of time that a nucleosomal DNA target site acts as though it is naked DNA (Fig. 1). The original method determined K_{equ} by determining the initial rates of cleavage of nucleosomal DNA relative to cleavage of naked DNA. The digestions occur in a rapid preequilibrium regime, in which

$$K_{equ} = \frac{(k_{mononucleosome})([RE]_{naked\ DNA})}{(k_{naked\ DNA})([RE]_{mononucleosome})}$$

where $k_{mononucleosome}$ and $k_{naked\ DNA}$ are observed pseudo-first-order rate constants for digestion of mononucleosomes and naked DNA, respectively, and $[RE]_{mononucleosome}$ and $[RE]_{naked\ DNA}$ are the concentrations of RE used in those respective digestions.

In the present study, we sought to quantify the effects of adding nucleosome neighbors with concomitant folding of the resulting chromatin fiber. Thus, we measured K_{equ} of site exposure for a unique target site in a nucleosome array relative to exposure of the same site in mononucleosomes, which we defined as follows:

$$K_{\text{relative-equ}} = \frac{K_{equ}^{array}}{K_{equ}^{mononucleosome}} = \frac{(k_{array})([RE]_{mononucleosome})}{(k_{mononucleosome})([RE]_{array})}.$$

We assumed here that the rates k_{23} and k_4 (Fig. 1) are the same for a test nucleosome in the middle of an array and for a single nucleosome. In reality, nucleosomal DNA that partially unwraps in the middle of an array is constrained at both ends, while in single nucleosomes, it is constrained at only one end. This constraint could alter the rate of binding k_{23} and/or the rate of cleavage k_4. Given the lengths of unwrapped DNA involved (unwrapping of ~80 bp suffices to provide unhindered access even to the middle of the nucleosome, with shorter unwrapping lengths required for sites nearer the ends of the nucleosome), this is not likely to be a dramatic effect, since the DNA is relatively stiff on that length scale. In fact, the modest differences in relative equilibrium constants that we do detect may, in part, be due to this difference. This does not change the overall interpretation of our results because the effects on accessibility of nucleosomal DNA from adding neighbors to a single nucleosome are very small in comparison with the large effects of wrapping the DNA into a nucleosome in the first place.

We determined $K_{\text{relative-equ}}$ by measuring the observed pseudo-first-order rates of cleavage of unique RE target sites in nucleosome arrays and in mononucleosomes k_{array} and $k_{mononucleosome}$ by six separate REs: PstI, HindIII, HaeIII, BamHI, StyI, and PmlI. The reactions were done by digesting both the purified nucleosome arrays and the mononucleosomes at 1 nM concentration in the appropriate enzyme buffer in a volume of 100 μl in the recommended NEB buffer. NEBuffer 1 contains 10 mM Bis-Tris propane–HCl, 10 mM $MgCl_2$, and 1 mM dithiothreitol. NEBuffer 2 contains 50 mM NaCl, 10 mM Tris–HCl, 10 mM $MgCl_2$, and 1 mM dithiothreitol. NEBuffer 3 contains 100 mM NaCl, 50 mM Tris–HCl, 10 mM $MgCl_2$, and 1 mM dithiothreitol. NEBuffer 4 contains 50 mM potassium acetate, 20 mM Tris–acetate, 10 mM magnesium acetate, and 1 mM dithiothreitol. BamHI buffer contains 150 mM NaCl, 10 mM Tris–HCl, 10 mM $MgCl_2$, and 1 mM dithiothreitol. Bovine serum albumin was added when recommended by NEB. The concentration of RE was used so that the glycerol concentration was at 5%, which maximized enzyme concentration without introducing "star" activity and is first order in enzyme concentration. In preliminary studies, we found that the cleavage rates of DNA within a nucleosome array and a mononucleosome are similar. Thus, we could improve the quantitative accuracy of the data by simultaneous measurement of relative cleavage rates on nucleosome arrays and mononucleosomes in the same reaction at the same time. This ensured that $[RE]_{mononucleosome}/[RE]_{array} = 1$.

Relative rates of cleavage were determined by quenching 10-μl aliquots taken at 1, 2, 4, 8, 16, 24, 32, and 40 min of digestion, by addition of EDTA to a final concentration of 20 mM. We separately confirmed the adequacy of the quench procedure by reactions in which we added EDTA prior to the RE. The quenched reaction aliquots were digested with 1 mg ml^{-1} of proteinase K plus 0.02% (w/v) SDS for 20 min at 50 °C to remove the histone proteins. The resulting DNA was then run on 5% native polyacrylamide gel, dried, and quantified using PhosphorImager and Image Quant software. There is an initial drop in undigested DNA following the first time point. This is due to the 5%–10% of nucleosomes that fall apart during the rapid mixing at the beginning of the digestions (see below). We ignore this initial time point, as was done in previous studies,[21,22] since the rapid drop in undigested DNA is due to digestion of naked DNA.

RE kinetics method for linker DNA

The RE kinetics method was also used to determine the equilibrium constant for site exposure in the linker region, in this case measured relative to cleavage of naked DNA. The equilibrium constant K_{equ} is defined as follows:

$$K_{equ} = \frac{(k_{\text{linker DNA}})([RE]_{\text{naked DNA}})}{(k_{\text{naked DNA}})([RE]_{\text{linker DNA}})}.$$

The observed rates of cleavage, $k_{\text{linker DNA}}$ and $k_{\text{naked DNA}}$, were determined as described above. The rates of digestion in the linker region of nucleosome arrays and in naked DNA were similar enough that they were done in the same reaction at the same time (thus, $[RE]_{\text{naked DNA}}/[RE]_{\text{linker DNA}} = 1$).

Nucleosome association

The RE digests were carried out in buffers that contain 10 mM Mg^{2+}, which can induce a reversible self-association (aggregation) of individual nucleosomes and of nucleosome arrays. This fact raises a question of whether such association influenced the observed site exposure equilibrium constants. Our results show that linker DNA sites in the nucleosome arrays are digested to completion in single exponential processes (Fig. 7) and that accessibility at some sites in the linker DNA is strongly influenced by the presence of neighboring nucleosomes, while accessibility at other sites is not. Moreover, we found that nucleosome arrays are digested inside the test nucleosome with overall rates that are close to those for digestion of individual nucleosomes. Each of these observations implies that most of the arrays must be participating in the RE digestions, since, if association rendered many of the nucleosome arrays inaccessible to RE digestion, the remaining fraction of the arrays would need to be digested at a correspondingly faster rate to give an effective rate that appears similar to single nucleosomes, which is not plausible. Together, these facts exclude the possibility that self-association creates bulk precipitation or heterogeneity in the sample or that association significantly influenced the measured relative equilibrium accessibilities.

Histone octamer disassociation

Rapid mixing of the nucleosome arrays with the RE causes up to 10% of the nucleosomes to fall apart,[21,38] which is responsible for a rapid initial drop in uncut DNA, as is seen for both dimer and 17-mer arrays (Fig. 6). We corrected for this behavior by omitting the first digestion time point from the kinetic analysis. Several facts argue that this loss of nucleosomes does not alter our measured equilibrium measurements. First, the nucleosome that is lost is almost always the test nucleosome (mp2) itself, because it has more sequence changes deviating from the selected high-affinity sequence (601) at key locations[2] than do the flanking (mp1) nucleosomes: mp1 has 8 base pair changes, while mp2 has 15; also, 2 of the base pair changes

in mp2 remove key TA dinucleotide steps, which are known to be critical for histone octamer affinity and nucleosome positioning. Therefore, the mp1 site is more stable and should have less histone octamer dissociation during the rapid mixing with the RE. This is confirmed by digesting with MluI, which cuts in the mp1 site but not the mp2 site. We found that only 3% of the mp1 sites lose their histone octamer during the digestions (Fig. 4c and d) as compared with 10% for the mp2 site. In summary, the most likely nucleosome to be lost upon initial mixing of the reaction is mp2. With the enzyme concentrations used in these experiments, the naked DNA thus created is digested instantly; we corrected for this by eliminating the first digestion time point from the kinetic analysis.

A second way through which nucleosome loss could influence the measured relative accessibilities is if the lost nucleosome happened to be adjacent to the test nucleosome, in which case we would be looking into the accessibility of a test nucleosome that did not, in fact, have an immediate neighbor on at least one side. Since only ~3% of flanking nucleosomes are lost, yet nucleosomes in arrays are digested at total rates that are similar to those for single nucleosomes, it follows that all the nucleosome arrays are participating in the digestion and that the measurements are overwhelmingly dominated by complete nucleosome arrays. If we assumed instead that the digestion is due to arrays with a missing nucleosome neighboring the test nucleosome, then the rates we report would not be normalized correctly, since only 6% of the arrays are missing one or the other flanking nucleosome. The actual digestion rates for the nucleosome arrays would need to be >16 (1/0.06) times faster than those for single nucleosomes for the total digestion rates to be similar. This would imply that the lack of a neighboring nucleosome increases the DNA accessibility by over 16-fold as compared with single nucleosomes—which is not plausible. For these reasons, we conclude that our results properly measure the actual relative equilibrium constants for DNA site exposure for nucleosomes surrounded by nucleosome neighbors.

Acknowledgements

We thank members of the Widom and Langowski labs for useful discussions and the Keck Biophysics Facility at Northwestern University for use of instruments. M.G.P. acknowledges support from the U.S. National Institutes of Health through postdoctoral fellowship F32 GM072306 and a Career Award in the Biomedical Sciences from the Burroughs Wellcome Fund. J.W. acknowledges research support from the U.S. National Institutes of Health through grants R01 GM54692 and R01 GM58617.

Supplementary Data

Supplementary data associated with this article can be found, in the online version, at doi:10.1016/j.jmb.2008.04.025

References

1. Richmond, T. J. & Davey, C. A. (2003). The structure of DNA in the nucleosome core. *Nature*, **423**, 145–150.
2. Segal, E., Fondufe-Mittendorf, Y., Chen, L., Thastrom, A., Field, Y., Moore, I. K. *et al.* (2006). A genomic code for nucleosome positioning. *Nature*, **442**, 772–778.
3. Almer, A., Rudolph, H., Hinnen, A. & Horz, W. (1986). Removal of positioned nucleosomes from the yeast PHO5 promoter upon PHO5 induction releases additional upstream activating DNA elements. *EMBO J.* **5**, 2689–2696.
4. Belikov, S., Gelius, B., Almouzni, G. & Wrange, O. (2000). Hormone activation induces nucleosome positioning *in vivo*. *EMBO J.* **19**, 1023–1033.
5. Boeger, H., Griesenbeck, J., Strattan, J. S. & Kornberg, R. D. (2003). Nucleosomes unfold completely at a transcriptionally active promoter. *Mol. Cell*, **11**, 1587–1598.
6. Fragoso, G., John, S., Roberts, M. S. & Hager, G. L. (1995). Nucleosome positioning on the MMTV LTR results from the frequency-biased occupancy of multiple frames. *Genes Dev.* **9**, 1933–1947.
7. Jack, R. S. & Eggert, H. (1990). Restriction enzymes have limited access to DNA sequences in *Drosophila* chromosomes. *EMBO J.* **9**, 2603–2609.
8. Lee, W., Tillo, D., Bray, N., Morse, R. H., Davis, R. W., Hughes, T. R. & Nislow, C. (2007). A high-resolution atlas of nucleosome occupancy in yeast. *Nat. Genet.* **39**, 1235–1244.
9. Sekinger, E. A., Moqtaderi, Z. & Struhl, K. (2005). Intrinsic histone–DNA interactions and low nucleosome density are important for preferential accessibility of promoter regions in yeast. *Mol. Cell*, **18**, 735–748.
10. Felsenfeld, G. (1996). Chromatin unfolds. *Cell*, **86**, 13–19.
11. Felsenfeld, G. & Groudine, M. (2003). Controlling the double helix. *Nature*, **421**, 448–453.
12. Kornberg, R. D. & Lorch, Y. (1999). Chromatin-modifying and -remodeling complexes. *Curr. Opin. Genet. Dev.* **9**, 148–151.
13. Kornberg, R. D. & Lorch, Y. (1999). Twenty-five years of the nucleosome, fundamental particle of the eukaryote chromosome. *Cell*, **98**, 285–294.
14. Saha, A., Wittmeyer, J. & Cairns, B. R. (2006). Chromatin remodelling: the industrial revolution of DNA around histones. *Nat. Rev. Mol. Cell Biol.* **7**, 437–447.
15. Smith, C. L. & Peterson, C. L. (2005). ATP-dependent chromatin remodeling. *Curr. Top. Dev. Biol.* **65**, 115–148.
16. Narlikar, G. J., Fan, H. Y. & Kingston, R. E. (2002). Cooperation between complexes that regulate chromatin structure and transcription. *Cell*, **108**, 475–487.
17. Peterson, C. L. & Logie, C. (2000). Recruitment of chromatin remodeling machines. *J. Cell. Biochem.* **78**, 179–185.
18. Kingston, R. E. & Narlikar, G. J. (1999). ATP-dependent remodeling and acetylation as regulators of chromatin fluidity. *Genes Dev.* **13**, 2339–2352.
19. Li, G., Levitus, M., Bustamante, C. & Widom, J. (2005). Rapid spontaneous accessibility of nucleosomal DNA. *Nat. Struct. Mol. Biol.* **12**, 46–53.
20. Li, G. & Widom, J. (2004). Nucleosomes facilitate their own invasion. *Nat. Struct. Mol. Biol.* **11**, 763–769.
21. Polach, K. J. & Widom, J. (1995). Mechanism of protein access to specific DNA sequences in chromatin: a dynamic equilibrium model for gene regulation. *J. Mol. Biol.* **254**, 130–149.
22. Anderson, J. D. & Widom, J. (2000). Sequence- and position-dependence of the equilibrium accessibility of nucleosomal DNA target sites. *J. Mol. Biol.* **296**, 979–987.
23. Polach, K. J. & Widom, J. (1996). A model for the cooperative binding of eukaryotic regulatory proteins to nucleosomal target sites. *J. Mol. Biol.* **258**, 800–812.

24. Miller, J. A. & Widom, J. (2003). Collaborative competition mechanism for gene activation *in vivo*. *Mol. Cell. Biol.* **23**, 1623–1632.
25. Vashee, S., Melcher, K., Ding, W. V., Johnston, S. A. & Kodadek, T. (1998). Evidence for two modes of cooperative DNA binding *in vivo* that do not involve direct protein–protein interactions. *Curr. Biol.* **8**, 452–458.
26. Vashee, S., Willie, J. & Kodadek, T. (1998). Synergistic activation of transcription by physiologically unrelated transcription factors through cooperative DNA-binding. *Biochem. Biophys. Res. Commun.* **247**, 530–535.
27. Bernstein, B. E., Liu, C. L., Humphrey, E. L., Perlstein, E. O. & Schreiber, S. L. (2004). Global nucleosome occupancy in yeast. *Genome Biol.* **5**, R62.
28. Bucceri, A., Kapitza, K. & Thoma, F. (2006). Rapid accessibility of nucleosomal DNA in yeast on a second time scale. *EMBO J.* **25**, 3123–3132.
29. Gottschling, D. E. (1992). Telomere-proximal DNA in *Saccharomyces cerevisiae* is refractory to methyltransferase activity *in vivo*. *Proc. Natl Acad. Sci. USA*, **89**, 4062–4065.
30. Loo, S. & Rine, J. (1994). Silencers and domains of generalized repression. *Science*, **264**, 1768–1771.
31. Chen, L. & Widom, J. (2005). Mechanism of transcriptional silencing in yeast. *Cell*, **120**, 37–48.
32. Lowary, P. T. & Widom, J. (1998). New DNA sequence rules for high affinity binding to histone octamer and sequence-directed nucleosome positioning. *J. Mol. Biol.* **276**, 19–42.
33. Dorigo, B., Schalch, T., Bystricky, K. & Richmond, T. J. (2003). Chromatin fiber folding: requirement for the histone H4 N-terminal tail. *J. Mol. Biol.* **327**, 85–96.
34. Dorigo, B., Schalch, T., Kulangara, A., Duda, S., Schroeder, R. R. & Richmond, T. J. (2004). Nucleosome arrays reveal the two-start organization of the chromatin fiber. *Science*, **306**, 1571–1573.
35. Huynh, V. A., Robinson, P. J. & Rhodes, D. (2005). A method for the *in vitro* reconstitution of a defined "30 nm" chromatin fibre containing stoichiometric amounts of the linker histone. *J. Mol. Biol.* **345**, 957–968.
36. Robinson, P. J., Fairall, L., Huynh, V. A. & Rhodes, D. (2006). EM measurements define the dimensions of the "30-nm" chromatin fiber: evidence for a compact, interdigitated structure. *Proc. Natl Acad. Sci. USA*, **103**, 6506–6511.
37. Ushinsky, S. C., Bussey, H., Ahmed, A. A., Wang, Y., Friesen, J., Williams, B. A. & Storms, R. K. (1997). Histone H1 in *Saccharomyces cerevisiae*. *Yeast*, **13**, 151–161.
38. Polach, K. J. & Widom, J. (1999). Restriction enzymes as probes of nucleosome stability. *Methods Enzymol.* **304**, 278–298.
39. Jason, L. J., Moore, S. C., Ausio, J. & Lindsey, G. (2001). Magnesium-dependent association and folding of oligonucleosomes reconstituted with ubiquitinated H2A. *J. Biol. Chem.* **276**, 14597–14601.
40. Yuan, G. C., Liu, Y. J., Dion, M. F., Slack, M. D., Wu, L. F., Altschuler, S. J. & Rando, O. J. (2005). Genome-scale identification of nucleosome positions in *S. cerevisiae*. *Science*, **309**, 626–630.
41. Belikov, S., Holmqvist, P. H., Astrand, C. & Wrange, O. (2004). Nuclear factor 1 and octamer transcription factor 1 binding preset the chromatin structure of the mouse mammary tumor virus promoter for hormone induction. *J. Biol. Chem.* **279**, 49857–49867.
42. Lee, C. K., Shibata, Y., Rao, B., Strahl, B. D. & Lieb, J. D. (2004). Evidence for nucleosome depletion at active regulatory regions genome-wide. *Nat. Genet.* **36**, 900–905.
43. Lomvardas, S. & Thanos, D. (2001). Nucleosome sliding by TBP binding *in vivo*. *Cell*, **106**, 685–696.
44. Roth, S. Y., Dean, A. & Simpson, R. T. (1990). Yeast alpha 2 repressor positions nucleosomes in TRP1/ARS1 chromatin. *Mol. Cell. Biol.* **10**, 2247–2260.
45. Anderson, J. D., Lowary, P. T. & Widom, J. (2001). Effects of histone acetylation on the dynamic equilibrium accessibility of nucleosomal DNA target sites. *J. Mol. Biol.* **307**, 977–985.
46. Polach, K. J., Lowary, P. T. & Widom, J. (2000). Effects of core histone tail domains on the equilibrium constants for dynamic DNA site accessibility in nucleosomes. *J. Mol. Biol.* **298**, 211–223.
47. Shogren-Knaak, M., Ishii, H., Sun, J. M., Pazin, M. J., Davie, J. R. & Peterson, C. L. (2006). Histone H4-K16 acetylation controls chromatin structure and protein interactions. *Science*, **311**, 844–847.
48. Schalch, T., Duda, S., Sargent, D. F. & Richmond, T. J. (2005). X-ray structure of a tetranucleosome and its implications for the chromatin fibre. *Nature*, **436**, 138–141.
49. Van Holde, K. E. (1989). *Chromatin.* Springer-Verlag, New York, NY.
50. Goldmark, J. P., Fazzio, T. G., Estep, P. W., Church, G. M. & Tsukiyama, T. (2000). The Isw2 chromatin remodeling complex represses early meiotic genes upon recruitment by Ume6p. *Cell*, **103**, 423–433.
51. Lomvardas, S. & Thanos, D. (2002). Modifying gene expression programs by altering core promoter architecture. *Cell*, **110**, 261–271.
52. Martinez-Campa, C., Politis, P., Moreau, J. L., Kent, N., Goodall, J., Mellor, J. & Goding, C. R. (2004). Precise nucleosome positioning and the TATA box dictate requirements for the histone H4 tail and the bromodomain factor Bdf1. *Mol. Cell*, **15**, 69–81.
53. Kagalwala, M. N., Glaus, B. J., Dang, W., Zofall, M. & Bartholomew, B. (2004). Topography of the ISW2–nucleosome complex: insights into nucleosome spacing and chromatin remodeling. *EMBO J.* **23**, 2092–2104.
54. Mutskov, V., Gerber, D., Angelov, D., Ausio, J., Workman, J. & Dimitrov, S. (1998). Persistent interactions of core histone tails with nucleosomal DNA following acetylation and transcription factor binding. *Mol. Cell. Biol.* **18**, 6293–6304.
55. Feng, H.-P., Scherl, D. S. & Widom, J. (1993). Lifetime of the histone octamer studied by continuous-flow quasielastic light scattering: test of a model for nucleosome transcription. *Biochemistry*, **32**, 7824–7831.
56. Thåström, A., Lowary, P. T. & Widom, J. (2004). Measurement of histone–DNA interaction free energy in nucleosomes. *Methods*, **33**, 33–44.